Terra Antartica
1998, **5**(3), 401-409

Origin of Breccias in the CRP-1 Core

S. PASSCHIER, T.J. WILSON & T.S. PAULSEN

Department of Geological Sciences and Byrd Polar Research Center, The Ohio State University, 275 Mendenhall, 125 South Oval Mall, Columbus OH 43210 - USA

Received 20 July 1998; *accepted in revised form* 15 October 1998

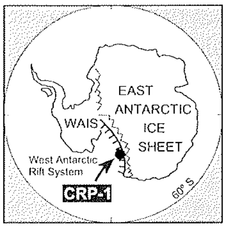

Abstract - CoreScan images were examined to determine the origin of breccias in the CRP-1 core. Breccias occur throughout the core, but are dominant deformation features in the upper 85 m. Breccia textures, boundaries and texture arrangements suggest that *in situ* fracturing and horizontal planar shearing are important deformation mechanisms in the upper part of the Miocene section. Forceful injections of silt and clay into fractures point to dewatering of overpressurised sediment. Breccias located below 55 metres below the sea floor (mbsf) occur associated with soft-sediment deformation, which is absent in younger intervals of the core. Deformation styles interpreted from the breccia textures, their downcore distribution, and the relations of breccias with sequence boundaries and lithologies, such as diamictites and graded beds, suggest brecciation occurred as a result of subglacial shearing and mass-movement processes. These mechanisms were also proposed for breccias and soft sediment deformation features observed in other McMurdo Sound cores. Subglacial shearing was a possible cause for the development of two thick brecciated intervals at ~44 and at ~79 mbsf, whereas slope failure and redeposition was probably the cause of brecciation below ~85 mbsf.

INTRODUCTION

The CRP-1 core was drilled on a bathymetric high, Roberts Ridge, 10-15 km off Cape Roberts, in northern McMurdo Sound, western Ross Sea (Cape Roberts Science Team, 1998a). Drilling sampled a gently tilted sequence on the margin of the Victoria Land Basin, one of four major extensional basins within the Ross Sea continental shelf. The drillsite is located on the western side of Roberts Ridge, which rises from a depth of 500 m below sea level in the west to less than a 100 m near the drillsite. Slopes on the northern and western sides of Roberts Ridge are steep, probably due to structurally controlled glacial erosion of the 900 m deep Mackay Sea Valley (Cape Roberts Science Team, 1998a). The regional area was glacierised during the time span represented by the core material, and the drillsite location may have been overridden by glaciers repeatedly (Barrett, 1986, 1989).

The CRP-1 core consists of a Quaternary glacigenic interval down to 43.55 metres below the sea floor (mbsf) and an early Miocene glacigenic interval down to the base of the core at 147.69 mbsf. Diamictites, sandstones, and siltstones are the main lithologies. The Quaternary section is composed of unconsolidated strata, the upper part of the Miocene section is composed of semi-consolidated strata, and the lower part of the Miocene section is largely composed of lithified strata. Numerous enigmatic brecciated intervals occur throughout the CRP-1 core, but are dominant between ~40 and ~85 mbsf in the lower Quaternary and the upper Miocene sections.

Breccias and soft-sediment deformation features were encountered in the CIROS-1 and the MSSTS-1 drillcores from further south in McMurdo Sound. In the MSSTS-1 core the deformation features were interpreted as the result of subglacial deformation (Barrett & McKelvey, 1986); in the CIROS-1 core they were attributed to mass-gravity flows (Hambrey et al., 1989). Upon the completion of drilling at Cape Roberts considerable debate remained about the origin of breccias that occur within the CRP-1 core. Did the breccias originate by *e.g.* tectonic, glacio-tectonic, mass-gravity or periglacial processes (*cf.* Laznicka, 1988)? We used scanned images of the slabbed core to characterise breccia textures, with the purpose of providing information on the physical processes of deformation. We conclude that brecciation occurred by *in situ* fracturing and by horizontal planar shearing in subglacial and mass-movement settings (Dreimanis, 1993; Hart & Roberts, 1994).

METHODOLOGY

After splitting of the CRP-1 core at the drillsite, the slabbed face of the working half of the core was scanned at a resolution of 5 pixels/mm using CoreScan® equipment leased from DMT, Germany. CoreScan images were inspected at The Ohio State University to describe breccia textures, other deformation features, and the relations between breccia occurrences, unconformities and lithological boundaries. The depths used in this paper are as initially determined at the drill site and as reported on the CoreScan images. Depths below 45.28 mbsf are the same as the ones used on the 1:20 Core Logs published in the Initial Report (Cape Roberts Science Team, 1998c). Sediment-filled fractures were examined in two thin sections, taken from ~44 and ~46 mbsf.

BRECCIA CHARACTERISTICS

TEXTURES

Brecciated sediments consist of multiple stacked zones of alternating textures. The textures range in thickness from several centimetres up to several decimetres, but never exceed a metre. We classified breccias based on textural criteria, generally following Laznicka (1988). Five breccia types were identified and include:

1) *crackle breccias*, which are defined as fracturing of the rock, in which no displacement of the fragments has occurred; the fragments are angular to subangular pebbles (Hambrey et al., 1997), and fit together in a jigsaw puzzle pattern (Fig. 1c);
2) *mosaic breccias* are similar to crackle breccias, but differ in that the fractures have been filled with sediment matrix;
3) *chaotic breccias* are defined as a mixture of large fractured pebbles in a groundmass of smaller fragments (Fig. 1b);
4) *rubble breccias* are defined as a mixture of subrounded, small pebbles, with irregular intergranular spaces (Fig. 1a); and
5) *matrix-supported breccias* consist of pebbles surrounded by a fine-grained matrix (Fig. 1d).

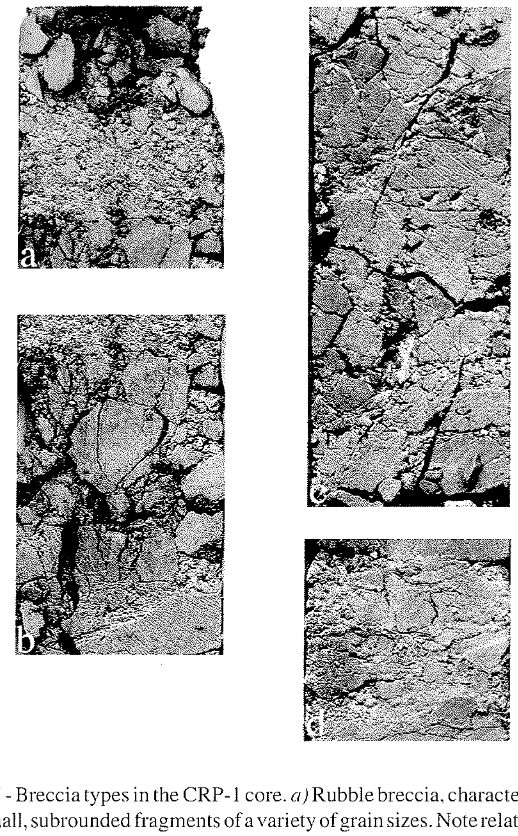

Fig. 1 - Breccia types in the CRP-1 core. *a)* Rubble breccia, characterised by small, subrounded fragments of a variety of grain sizes. Note relatively abrupt change to smaller grain size of rubble breccia across planar boundaries with chaotic breccia above and below. *b)* Chaotic breccia, with large, fractured clasts intermixed with fine-grained brecciated material. *c)* Crackle breccia, characterized by network of cracks separating angular fragments that have not been displaced. *d)* Matrix-supported breccia, with pebble-sized fragments surrounded by a fine-grained matrix. Core diameter is 61 mm.

BOUNDARIES

Boundaries between breccias and non-brecciated zones within a breccia interval are either sharp or gradational. Sharp and gradational boundaries are commonly observed in the same brecciated interval (Fig. 2c). Most boundaries between different breccia types within brecciated intervals are horizontal and planar. Irregular and inclined boundaries are rare (Fig. 2a & b). Sharp and planar boundaries typically separate rubble breccias from adjacent crackle breccias. Lower boundaries of brecciated intervals are as commonly irregular as they are planar.

THICKNESS AND INTERNAL ARRANGEMENT OF BRECCIATED ZONES

The thickness of brecciated intervals ranges from 8 to 635 cm. In two cases, brecciated intervals reach ~6 m thickness and consist of multiple zones of alternating breccia types (Figs. 2c & 3). Brecciated zones within breccia intervals appear to be horizontal tabular bodies, based on their subhorizontal upper and lower boundaries. In the upper 85 m of the core, the lower sections of brecciated intervals consist of crackle breccias. Crackle breccia zones also occur as layers within intervals dominated by rubble and matrix-supported breccias, *e.g.* in figure 3 between ~49 and ~50 mbsf and in figure 4 at 69.55 mbsf. Mosaic breccias typically grade into crackle breccias. Crackle breccias commonly grade into chaotic, rubble and matrix-supported breccias.

COMPOSITION OF BRECCIA FRAGMENTS, SEDIMENT MATRIX, AND SEDIMENT-FILLED CRACKS

The breccias occur in lithologies ranging from clayey siltstone to silty fine sandstone, except for the breccia in Quaternary strata, which occurs in diamicton. In all cases the composition of the breccia clasts is the same as the host rock, indicating that the breccias are intraformational. The sediment matrix surrounding the breccia clasts is generally lighter in colour, but of the same lithological composition (Fig. 1d). Sediment-filled cracks of mosaic breccias are abundant in the upper part of the Miocene section, commonly directly associated with crackle breccias. Thin section observations indicate that, locally, the sediment fill in cracks is graded, with a wall-parallel stratification of silt and clay (Fig. 5). The clay particles have a common extinction angle under crossed polarizers, suggesting that clay particles are aligned parallel to the crack wall. Carbonate cement and microconcretions are also present in intergranular spaces and cracks (see Baker & Fielding, this volume). In addition to the sediment-filled cracks two clastic dykes occur in the CRP-1 core: one at 133.52 to 133.77 m, and one at 139.05 to 139.31 m. The dykes are approximately 1.5 cm wide and have steep dips.

ASSOCIATION WITH OTHER DEFORMATION FEATURES

Planar fractures that cross-cut the core margins are abundant in the uppermost Miocene strata where

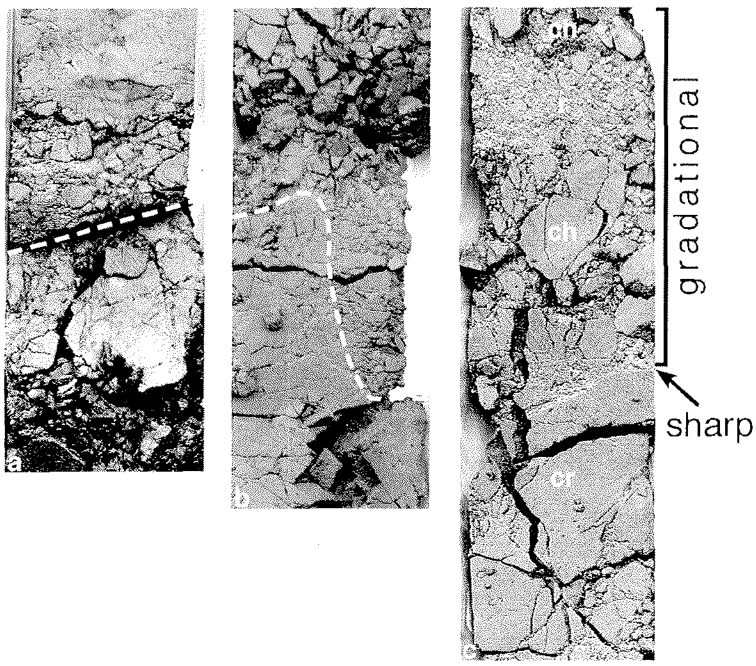

Fig. 2 - Boundaries between breccia types in the CRP-1 core.
a) Inclined boundary (white dashed line).
b) Irregular boundary (white dashed line).
c) Gradational and sharp boundaries. Most boundaries between breccia textures are sharp and planar. Note stacked nature of breccia types in 2c, where crackle breccia (cr) at base of interval passes upward into chaotic (ch) and rubble (r) breccias.
Core diameter is 61 mm.

brecciation is extensive, but elsewhere in the core there is no systematic correlation between high fracture abundance and the presence of brecciated intervals (see Fig. 2 in Wilson & Paulsen, this volume). A conjugate set of listric microfaults with normal displacement occurs at ~65-70 mbsf and a reverse fault was observed at ~109 mbsf. Below 55 mbsf, the breccias occur in association with soft-sediment folding (Fig. 6) and chaotic sediment mixing. Soft-sediment deformation is absent in the upper 55 m of the core.

BRECCIA SEQUENCE AND STRATIGRAPHIC BOUNDARIES

DOWNCORE SEQUENCE OF BRECCIAS

The breccias are confined to 10 intervals, which are described in table 1. Brecciation is most abundant between ~40 and ~85 mbsf, with only thin breccia intervals occurring below ~85 m (Fig. 7). The Quaternary section is poorly indurated and core recovery is low, so only one brecciated

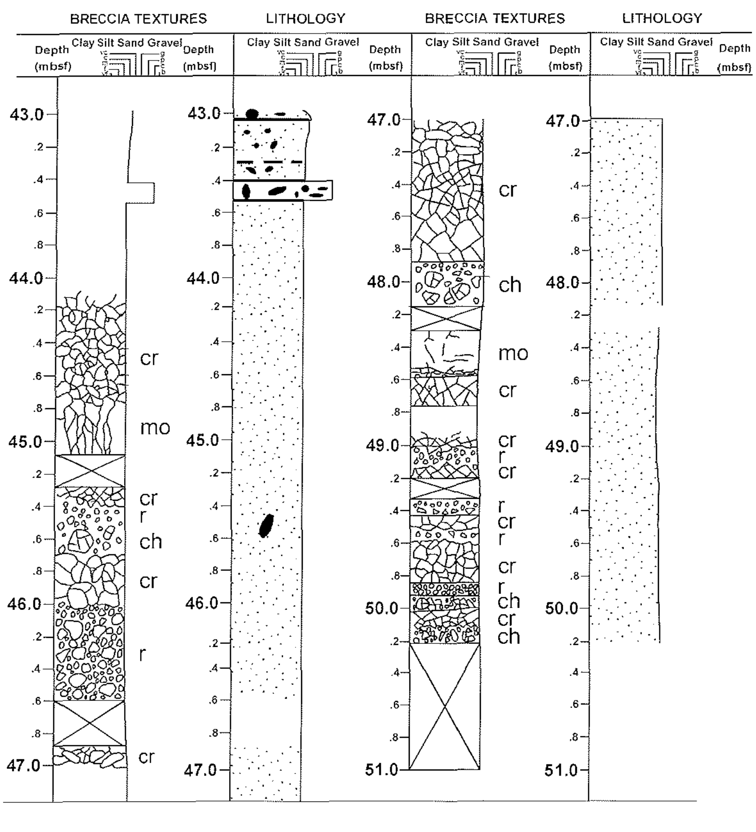

Fig. 3 - Detailed 1:20 log of breccia 2, below the Quaternary-Miocene boundary in CRP-1. (Key: cr=crackle, mo=mosaic, ch=chaotic, and r= rubble breccia.) Two types of associations are particularly common: 1) crackle breccias adjacent to rubble breccias with a sharp boundary in between the types; or, 2) crackle breccias grading upwards or downwards into chaotic textures with large fractured clasts in a rubbly groundmass, which in turn pass into rubble breccias. No changes in lithology occur at the boundaries between textures. The crackle breccias clearly represent *in situ* brecciation with minimal movement of clasts. The smaller and more rounded fragments in the rubble breccias point to grain-size reduction and abrasion of clasts, suggesting some degree of transport.

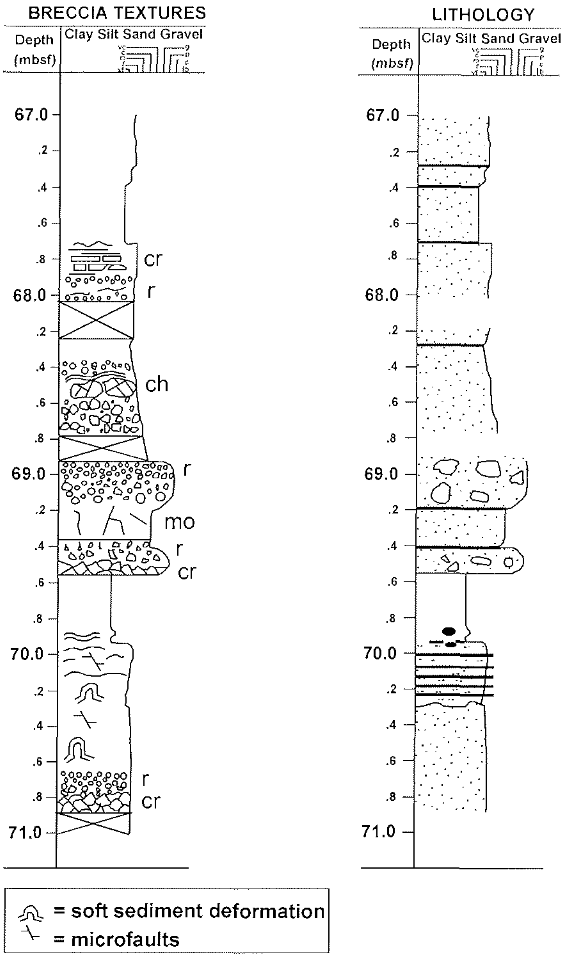

Fig. 4 - Detailed 1:20 log of breccia 4, CRP-1. (Key: cr=crackle, mo=mosaic, ch=chaotic, and r= rubble breccia.) Crackle breccias, indicative of *in situ* brecciation, are of minor importance. Local crackle breccias pass upwards into rubble and chaotic breccias, which grade into soft-sediment deformation features. Boundaries between breccia types in this interval are mainly gradational.

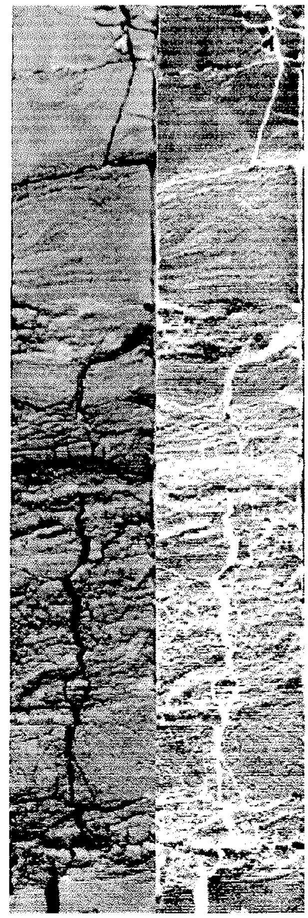

Fig. 6 - Soft-sediment deformation and brecciation at ~67 mbsf. Contorted lamination may represent soft-sediment folding, which is overprinted by brecciation (crackle breccia). The left side is a positive CoreScan image, the right side is a negative image of the same interval, where open cracks appear white, highlighting the breccia texture. Core diameter is 61 mm.

interval, which occurs within a diamicton, could be described with confidence. Crackle and mosaic breccias are dominant in the upper part of the Miocene section, above ~85 m, and are less common below this depth, where rubble and matrix-supported breccias are dominant.

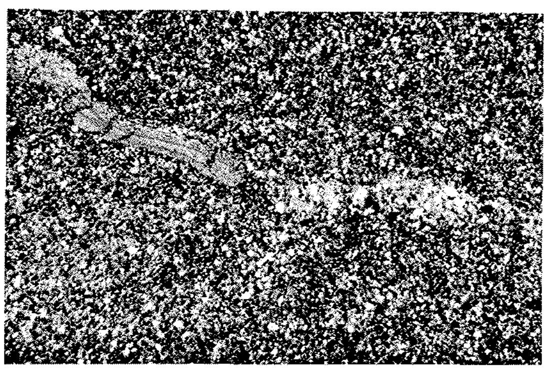

Fig. 5 - Thin section photomicrograph of sediment-filled crack at 44.49 - 44.64 mbsf. The sediment-filled crack is ~1 mm across. Note wall-parallel stratification and change in grain size of clastic fill along the length of the crack.

Two ~6 m thick breccia intervals occur in the upper part of the Miocene section (breccias 2 and 5). Breccias 2 (Fig. 3) and 5 contain numerous sharp, horizontal, planar boundaries, and breccia types occur in the following two arrangements: 1) crackle breccias adjacent to rubble breccias with a sharp boundary in between the types; or, 2) crackle breccias grading upwards or downwards into chaotic breccias with large fractured clasts in a rubbly groundmass, which in turn pass into rubble breccias (Figs. 2c & 3).

Breccia 1 is similar to breccia 2, but breccia 1 contains more discontinuous brecciation and is thinner. Clear planar horizons are not characteristic of breccias 3, 4, 6, 7, 8, 9 and 10, which have gradational boundaries and soft-sediment deformation between breccia types.

ASSOCIATION OF BRECCIAS WITH UNCONFORMITIES AND FACIES

Some breccias have developed just below sequence boundaries (Fig. 7), that have been defined based on rapid shifts in facies and grain-size (Fielding et al., this volume). The sequence boundaries at ~43 (the Quaternary-Miocene boundary), at ~79, ~92, and at ~116 mbsf overlie breccia 2, 5, 6 and 8, respectively. It is notable that the facies

Tab. 1 - Characterisation of breccias in CRP-1.

Breccia #	Depth (mbsf)	Thickness (cm)	Lithology	Dominant breccia textures	Boundaries	Other deformation	Sediment-filled cracks	Associated with breccia	Interpretation
1	40.35-41.79	144	diamicton	chaotic/ crackle	grad./sharp	-	-	diamicton	subglacial shear?
2	44.10-50.23	635	fine sandstone	crackle/ chaotic	sharp/grad.	fractures	abundant	diamictite	subglacial shear
3	55.95-58.45	250	coarse siltstone	chaotic/rubble	gradational	soft sed. def.	present	interstratified diamictite	slope failure
4	67.60-70.90	330	silty sandstone	rubble/chaotic	sharp/grad.	soft sed. def. fractures microfaults	-	diamictite	subglacial shear?
5	79.55-85.52	597	silty fine sandstone	rubble/crackle	sharp/grad.	soft sed. def.	abundant	diamictite w/microfabric	subglacial shear
6	92.44-92.52	8	mudstone	chaotic	grad./sharp	-	-	graded beds	slope failure
7	110.38-110.46	8	clayey siltstone	matrix-supported	gradational	soft sed. def. microfaults	present	laminated sediments	slope failure
8	116.22-116.48	26	sandy siltstone	chaotic	grad./sharp	soft sed. def.	-	interstratified diamictite	slope failure
9	118.19-119.30	111	silty v. fine sandstone	rubble/ matrix-sup.	gradational	soft sed. def.	-	laminated sediments	slope failure
10	147.32-147.47	15	fine sandstone	matrix-supported	sharp	-	-	bioturbation	slope failure

Note: grad.=gradational; soft sed. def.= soft sediment deformation.

associations that form the sequences in the lower part of the core are more complete than in the upper 85 m. It is interpreted that the advance stage of the glacial cycle is missing from the sequences between 40 and 85 mbsf (Powell et al., this volume), which suggests that glacial erosion took place. A break in sedimentation and erosion at the top of brecciated intervals may also be present in the lower part of the core. Shifts in magnetic susceptibility at 92, 110 and 116 mbsf coincide with the presence of breccias 6, 7 and 8 below these levels (Cape Roberts Science Team, 1998a).

Diamictites overlie sequence boundaries above breccias 1, 2, 3, 4, 5, and 8. Breccias 6, 7 and 9 occur above and below graded beds and stratified sediments.

BRECCIATION MECHANISMS

IN SITU BRECCIATION

Crackle and mosaic breccias comprise of a framework of angular and subangular clasts that show little or no evidence for displacement, suggesting that they formed by *in situ* fragmentation of the rock (Fig. 1c). In the core, crackle and mosaic breccias occur in discrete zones within intervals consisting of rubble textures and, in the lower part of the core, with soft-sediment deformation. At the top of breccia 5 (~79 mbsf), soft-sediment deformation structures point to chaotic mixing of sediment under high pore-fluid pressures. Sediment-filled cracks forming mosaic breccias occur throughout breccias 2 and 5. In breccia 2, the orientation of the clays and the wall-parallel stratification of the clastic infill of cracks suggest that they developed due to forceful injection of sediment. Sediment can become overpressured when it is subjected to a compressional stress regime. Fractures filled with sediment may have formed as tensional veins were injected by clastic material during dewatering of unconsolidated sediment. Conventional triaxial compression tests in experiments on a variety of isotropic rocks have shown that when a rock is loaded to failure extension fractures may develop in low strain situations (Hancock, 1985). The orientation of the extension fractures will be parallel to the maximum stress direction. A vertical load is consistent with the dominantly high-angle orientation of the sediment-filled veins in breccias 2 and 5. Collectively, the jigsaw puzzle morphology of the breccia textures, the presence of clastic vein injections, and their direct association with chaotic sediment mixing, suggest that *in situ* brecciation occurred as a response to release of high fluid pressures induced by a vertical load.

SHEAR-INDUCED BRECCIATION

The overall decrease in grain-size within tabular zones of chaotic, rubble and matrix-supported breccias suggests grain-size reduction by shear-related cataclasis. The subhorizontal, tabular geometry of the breccia intervals indicates failure of the sediment by horizontal shear along discrete planar zones. In breccia 2, the stacking and alternation of breccia textures indicate partitioning of strain between horizontal layers (Fig. 3). Two distinct shear-related deformation styles occur in breccias 2 and 4. Breccia 2 contains sharp boundaries between textures and abundant *in situ* brecciation (Fig. 3). Breccia 4 contains mostly rubbly textures grading into soft-sediment deformation (Fig. 4).

The textural characteristics, stacking of textures, tabular breccia geometries and planar boundaries, suggest a brittle shear model for the higher-level CRP-1 breccias. The presence of soft-sediment deformation features below 55 mbsf suggests that the sediments were not lithified during deformation. Since brittle shearing does not likely occur under high pore-water pressures in unlithified

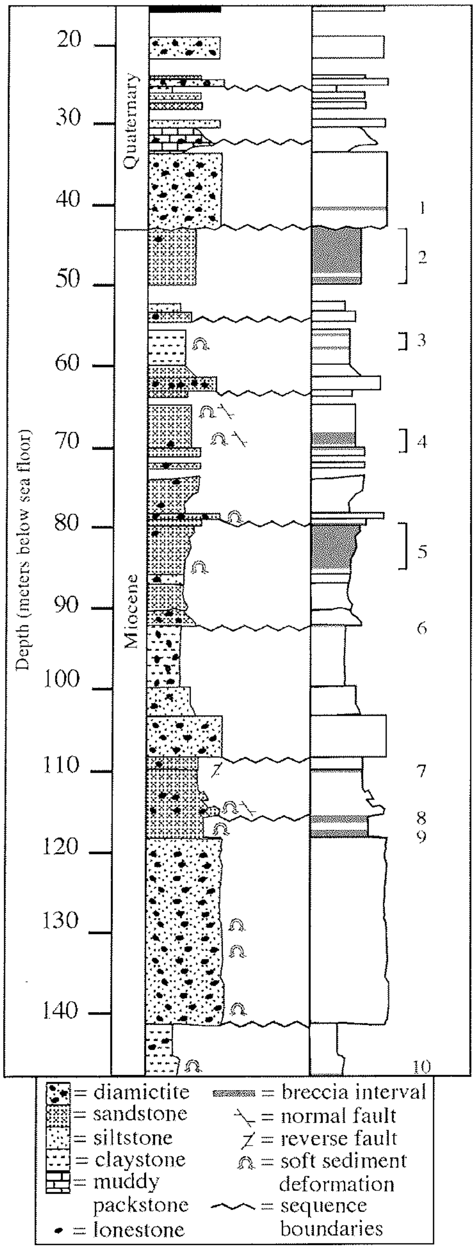

Fig. 7 - Downcore distribution of breccias and other deformation features in the CRP-1 core. Numbers denote breccia units discussed in the text and described in table 1. Lithologic log and sequence boundaries after Cape Roberts Science Team (1998b, 1998c). Note: single breccia in Quaternary section; association of thickest breccia units (2, 5) with sequence boundaries overlain by diamictites; and the association of brecciated intervals with other deformation features from 55 mbsf to the base of the core.

sediments, it probably postdates the dewatering of the sediment. Overall it appears that subhorizontal shear, with localisation of strain in discrete zones marked by matrix-supported and rubble breccias, accords with the macroscopic textural evidence in breccia 2.

Present data do not allow us to constrain why soft-sediment deformation occurs in association with brecciation below 55 mbsf, but is lacking above. The different deformation styles may be due to differences in applied stress or different mechanical properties of the sediment, due to factors such as pore-water pressure, the degree of lithification, or the frozen *vs.* unfrozen state of the sediment (Brodzikowski & Van Loon, 1985). Studies of brittle shear failure of indurated sandstones show that brecciation occurs during the initial stages of cataclasis (Hancock, 1985). However, brittle shear bands lacking ductile deformation features also develop in shear zones under subfreezing conditions (Echelmeyer & Wang, 1987).

MODELS FOR BRECCIA FORMATION

HYPOTHESES FOR THE ORIGIN OF THE BRECCIAS

Breccias are described from a variety of structural settings and depositional environments (Laznicka, 1988). To determine the origin of the breccias in the CRP-1 core, we examined the composition of the fragments and host rock, the geometry of the brecciated bodies and their boundaries, the presence of other deformation features and the association of breccias with stratigraphic boundaries. In the CRP-1 core, the breccias consist mainly of intraclasts (*i.e.* the breccias are intraformational) and they are commonly developed below sequence boundaries. Most brecciated zones in the core appear to comprise (sub)horizontal tabular bodies. Clastic injections and soft-sediment mixing indicate the presence of high water-pressure. Cleavage does not occur in the core. The absence of cleavage and the lack of exotic clasts eliminates a tectonic origin for the breccias. Cryostatic brecciation is associated with rapid changes in porosity and permeability of sediments (Brodzikowski & Van Loon, 1985; Menzies, 1990), which is not characteristic of breccias in the CRP-1 core. Further more, the sediments in the core were deposited in a marine environment, whereas cryostatic brecciation is mainly described from terrestrial settings (Laznicka, 1988). Cataclasis by brittle shearing, inferred here from textural evidence, is a mechanism which does not occur by freezing and thawing of sediment. The brecciated intervals do display a variety of textures, brecciation is discontinuous and associated with clastic injections, which is typical of syn-sedimentary breccias, such as those formed in subglacial environments and mass-movement settings (Brodzikowski & Van Loon, 1985; Peryt & Jasionowski, 1994). The position of brecciated intervals below sequence boundaries suggests that the brecciation may be related to the development of these boundaries.

Two possible models are thus considered likely for the formation of the breccias in the CRP-1 core: 1) subglacial deformation or 2) slope failure and resedimentation. Subglacial deformation is a plausible model for the origin of the breccias because deformation features similar to those described in subglacial shear zones occur in the CRP-1 core. Slope failure and resedimentation is also a plausible model because the Cape Roberts drill site is located on a steep slope of the Roberts Ridge. An important aspect in the characterisation of the core is to identify ice-grounding events. For this purpose we attempt to distinguish between deformation structures produced in a subglacial environment and a mass-gravity flow setting. Therefore, we examined textural arrangements and boundaries of individual brecciated intervals in the core, in combination with other sedimentological information, such as lithology, fabric, and primary sedimentary structures, to determine the applicability of these two models for the origin of the breccias.

SUBGLACIAL DEFORMATION OR SLOPE FAILURE AND RESEDIMENTATION?

Alternating textures over short intervals, sharp boundaries between horizons, and horizontal brittle and ductile shearing are features both observed in mass-movement settings and in glaciotectonised sediments. However, unique sedimentary and structural features of the two environments help to constrain models for the origin of the breccias (Brodzikowski & Van Loon, 1985; van der Meer, 1987; Dreimanis, 1993; Hart & Roberts, 1994; Peryt & Jasionowski, 1994; van der Wateren, 1995). Extension fractures filled with sediment are common in glaciotectonised sediments. Sheared sediment lenses are usually more sinuously curved in mass movement settings and more planar in subglacial environments. The association and interbedding of breccias and soft-sediment deformation structures with graded beds and sorted sediments with primary sedimentary structures is considered diagnostic for mass-gravity flow environments. If a basal till overlies deformed sediments, the deformation is likely to have been caused by glacial action.

BRECCIAS FORMED BY SUBGLACIAL DEFORMATION

Where diamictites overlie a brecciated zone (breccias 1, 2, 3, 5, 8), it is possible that the emplacement of the diamictite is related to the development of the breccia. Other evidence from the cored sequence, such as clast-fabric (Cape Roberts Science Team, 1998b) and microfabric studies (van der Meer, this volume) on diamictites, point to glacial overriding of the site. The Ross Sea continental shelf is part of the glaciated Antarctic continental margin with a thick sediment cover. Grounded ice at the location of the drillsite would possibly deform the underlying sediments. Deformation features similar to those described from subglacial shear zones in both temperate and frozen subglacial environments were encountered in the CRP-1 core; hence this seems a likely scenario for breccia formation.

Icesheets terminating on continental shelfs overlie sediment beds. The bed may be composed of a thin layer of basal diamict transported by the glacier, overlying sequences of strata deposited in either glacial or non-glacial environments. Studies in modern glacial environments have established the presence of deforming beds beneath many glaciers and ice-sheets (Boulton & Hindmarsh, 1987; Murray, 1997; Alley et al., 1997). Studies of Pleistocene glaciations in Europe have shown that ice acting on unconsolidated sediments can produce extensive deformation (van der Meer, 1987; van der Wateren, 1995; Boulton, 1996). Most deformation structures are the result of subglacial shear near the ice-margin, which occurs under both temperate and subfreezing conditions (Boulton, 1996; Echelmeyer & Wang, 1987). Besides breccias, soft-sediment folding, high-angle fractures and clastic injections are common in Pleistocene subglacial shear zones (Dreimanis, 1993; van der Wateren, 1995). Echelmeyer & Wang (1987) identified brittle shear bands and slip surfaces within a frozen basal debris layer beneath a modern Chinese glacier.

The two thick brecciated intervals, breccia 2 and 5, below the Quaternary-Miocene boundary and below ~79 mbsf, respectively, differ from other brecciated intervals by their thickness (~ 6 m), more *in situ* brecciation, and the abundance of sediment injections (Tab. 1). Both breccias have many sharp, internal boundaries, which may be slip planes. In breccia 5, a transition from crackle and mosaic breccias at the bottom to rubble and matrix-supported breccias at the top, suggest a change from more *in situ* brecciation at the bottom to horizontal shear-deformation at the top. A zone of soft-sediment mixing between the diamictite and the brecciated interval indicates high pore-water pressure in the sediment below the diamictite. The sediment injections point to dewatering of this sediment, which may have occurred as a response to a significant vertical load, such as grounded ice. This interpretation is supported by independent evidence for glacial overriding at ~79 m (above breccia 5) where microstructures in thin sections suggest that the diamictites at these levels have been tectonised (van der Meer, this volume). The position of breccia 2 below the Quaternary-Miocene boundary, a major unconformity that possibly developed as a result of glacial erosion, further suggests that brecciation is the product of subglacial deformation.

Considering the presence of high angle fractures, multiple slip planes, the thickness of the brecciated intervals and the association with unconformities, subglacial shearing was the likely cause of formation of breccias 2 (~ 43 m) and 5 (~ 79 m). These hypotheses should be tested by more research on thin sections of rubble breccias, to determine whether these zones show microscopic signs of shear deformation. Breccia 1 occurs within a clast-poor muddy diamictite in the Quaternary section. The internal arrangement and boundaries of breccia textures within the brecciated interval suggests horizontal brittle shearing took place. However, additional evidence for subglacial shearing is not available (Tab. 1). Breccia 4 occurs 3 m below a diamictite that contains a distinct clast fabric and microscopic evidence of deformation (van der Meer, this volume), suggesting glacial overriding. The presence of soft-sediment folding in breccia 4 suggests horizontal shearing under high pore-water conditions, which is characteristic of both a subglacial and gravity flow setting (Hart & Roberts, 1994). Thus, it is not clear whether the deposition of the diamictite is related to the brecciation in this case.

Other diamictites in the lower part of the core (at ~105, 123 and 134 mbsf) interpreted by van der Meer (this volume) to have been deformed, are not directly associated with breccias, which suggests that shear-induced brecciation took place under restricted conditions. It is possible that lithology plays an important role in breccia formation, because 9 out of 10 breccias in the CRP-1 core developed in fine sandstones and siltstones. These lithologies are not abundant in the lower part of the Miocene section, where thick breccias are lacking, but are abundant in the upper part of the Miocene section, where most breccias occur. The thickness of a deforming bed depends upon the lithology exposed beneath the ice-sheet (Boulton, 1996). Diamictites typically have low permeabilities because of their broad grain-size distribution. Sandstones and siltstones are more susceptible to brittle failure than diamictites, because the former are more permeable, resulting in lower pore-water pressures in the sediment. If pore-water pressures are high, the effective stress is reduced, and strain may be accounted for by ductile deformation of a relatively thin basal till. Brittle failure of underlying sandstones or siltstones results in dewatering of the basal till and an increase of the depth of deformation. Microfabrics are most distinct in the diamictites at 123 and 134 mbsf, where breccias are absent, and less pronounced in the upper part of the core where breccias dominate. In the diamictites in the lower part of the core described by van der Meer (this volume), localization of strain in a thin deforming bed may have occurred, because the underlying lithologies were impermeable enough to maintain high pore-water pressures and to prevent brittle failure of the sediment.

SLOPE FAILURE, RESEDIMENTATION

Slope failure occurs as a result of gravity pull on sediments. Sedimentation at a stable grounding line in a sub-Arctic environment tends to produce morainal banks with steep slopes on which mass movement is a common process (Powell & Molnia, 1989). Meltwater release and sediment deposition at the grounding line increase the gravitational instability of the proglacial environment. In the presence of high pore-water pressures, sediment deposition on a moderate slope can be sufficient to overcome the internal friction of the sediment. Earthquakes also trigger slope failure and are likely to have occurred in the Miocene tectonic setting, associated with rifting in the Ross Sea and uplift of the Roberts Ridge. *In situ* brecciation and matrix-supported breccias accompanied by soft-sediment deformation are characteristic of local slope failure in a water-saturated environment (Brodzikowski & Van Loon, 1985; Peryt & Jasionowski, 1994).

The diamictite above breccia 8 contains thin beds of sandstone, and the lithology overlying breccia 3 is interstratified diamictite, mudstone and sandstone, which suggests that these diamictites were redeposited. Breccia 6, 7 and 9 in the lower part of the core are associated with laminated sediments and graded beds (Tab. 1). Howe et al. (this volume) argue that distal gravity flows (turbidites) are present below 115 mbsf and that ice-proximal gravity flows are a possible explanation for the laminated sediments deposited between 90 and 115 mbsf. This is consistent with the nature of the breccias in this interval, which are thin chaotic and matrix-supported breccias with irregular boundaries. Breccia 10 has irregular boundaries and is matrix-supported, suggesting that it has also been redeposited.

SUMMARY AND CONCLUSIONS

Macroscopic observations of the breccias within the CRP-1 core suggest *in situ* fracturing, brittle shearing along discrete shear planes, and ductile deformation were associated with breccia formation in the CRP-1 strata. One breccia was formed during the Quaternary, one some time between the early Miocene and the Quaternary, and 8 breccias were formed in the early Miocene. The two types of settings in which brecciation is likely to have occurred are subglacial shearing and slope failure and resedimentation. This is similar to interpretations of breccias observed in other McMurdo Sound cores (Barrett & McKelvey, 1986; Hambrey et al. 1989).

Breccias 2 and 5 were most likely to have formed in a subglacial environment, based on multiple sediment-filled veins and brittle-shearing textures, the great thickness of the brecciated intervals and their association with unconformities and deformed diamictites. Breccias 1 and 4 may also have formed by subglacial shearing, but the textures are not as pronounced and the breccias do not directly relate to unconformities or deformed diamictites. Breccias 6, 7, 9 and 10 were probably formed in a mass-movement setting based on the characteristics of the textures (*e.g.* matrix-supported breccias) and their association with graded beds or stratified sediments. Breccias 3 and 8 are associated with interstratified diamictites, which suggests that they may have formed in an ice-proximal glaciomarine environment. Breccias below 55 m are accompanied by soft-sediment folding and mixing, which is absent above 55 mbsf. This change in deformation style may be related to the temperature and pore-water regime or to differences in the state of lithification of the strata during deformation.

ACKNOWLEDGEMENTS

M. Hambrey, J. van der Meer and an anonymous referee provided helpful comments, which greatly improved the manuscript. The core scanning was supported by NSF grant OPP-9527394 to T.J. Wilson. Christie Demosthenous and Bill Crotinger helped to produce the figures. Dr. G. Rafat generously volunteered his time and expertise for set up and training on the CoreScan. Fee waivers and software access provided by DMT facilitated this research.

REFERENCES

Alley R.B., Cuffey K.M., Evenson E.B., Straaser J.C., Lawson D.E. & Larson G.J., 1997. How glaciers entrain and transport basal sediment: physical constraints. *Quaternary Science Reviews*, **16**, 1017-1038.

Barrett P.J. (ed.), 1986. Antarctic Cenozoic history from the MSSTS-1 drillhole, McMurdo Sound. *DSIR Bulletin*, **237**, 174 p.

Barrett P.J. (ed.), 1989. Antarctic Cenozoic history from the CIROS-1 drillhole, McMurdo Sound. *DSIR Bulletin*, **245**, 254 p.

Barrett P.J. & McKelvey B.C., 1986. Stratigraphy. In: Barrett P.J. (ed.), *Antarctic Cenozoic history from the MSSTS-1 drillhole, McMurdo Sound, DSIR Bulletin*, **237**, 9-35.

Boulton G.S., 1996. Theory of glacial erosion, transport and deposition as a consequence of subglacial sediment deformation. *Journal of Glaciology*, **42**(140), 43-62.

Boulton G.S. & Hindmarsh R.C.A., 1987. Sediment deformation beneath glaciers: rheology and geological consequences. *Journal of Geophysical Research*, **92**(B9), 9059-9082.
Brodzikowsi, K. & Van Loon A.J., 1985. Penecontemporaneous non-tectonic brecciation of unconsolidated silts and muds. *Sedimentary Geology*, **41**, 269-282.
Cape Roberts Science Team, 1998a. Background to CRP-1, Cape Roberts Project, Antarctica. *Terra Antartica*, **5**(1), 1-30.
Cape Roberts Science Team, 1998b. Miocene Strata in CRP-1, Cape Roberts Project, Antarctica. *Terra Antartica*, **5**(1), 63-124.
Cape Roberts Science Team, 1998c. Appendix 2, 1:20 Core Logs. *Terra Antartica*, **5**(1), 141-175.
Dreimanis A., 1993. Small to medium-sized glacitectonic structures in till and in its substratum and their comparison with mass movement structures. *Quaternary International*, **18**, 69-79.
Echelmeyer K. & Wang Z., 1987. Direct observations of basal sliding and deformation of basal drift at subfreezing temperatures. *Journal of Glaciology*, **33**(113), 83-98.
Hambrey M.J., Barrett P.J. & Robinson P.H., 1989. Stratigraphy. In: Barrett P.J. (ed.), *Antarctic Cenozoic history from the CIROS-1 drillhole, McMurdo Sound, DSIR Bulletin*, **245**, 23-48.
Hambrey M.J. et al., 1997. Cape Roberts Project Core Logging Manual. *Antarctic Data Series*, **21**, Victoria University Wellington, 89 p.
Hancock P.L., 1985. Brittle microtectonics: principles and practice. *Journal of Structural Geology*, **7**(3/4), 437-457.
Hart J.K. & Roberts D.H., 1994. Criteria to distinguish between subglacial glaciotectonic and glaciomarine sedimentation, I. Deformation styles and sedimentology. *Sedimentary Geology*, **91**, 191-213.
Laznicka P., 1988. Breccias and Coarse Fragmentites-petrology, environments, associations, ores. *Developments in Economic Geology*, **25**, 832 p.
Menzies J., 1990. Brecciated diamictons from Mohawk Bay, S. Ontario. *Sedimentology*, **37**, 481-493.
Murray T., 1997. Assessing the paradigm shift: deformable glacier beds. *Quaternary Science Reviews*, **16**, 995-1016.
Peryt T.M. & Jasionowski M., 1994. *In situ* formed redeposited gypsum breccias in the Middle Miocene Badenian of southern Poland. *Sedimentary Geology*, **94**, 153-163.
Powell R.D. & Molnia B. F., 1989. Glacimarine sedimentary processes, facies and morphology of the south-east Alaska shelf and fjords. *Marine Geology*, **85**, 359-390.
van der Meer J.J.M. (ed.), 1987. *Tills and Glaciotectonics*. Balkema, Rotterdam, The Netherlands.
van der Wateren F.M., 1995. Structural geology and sedimentology of push moraines. *Mededelingen van de Rijks Geologische Dienst*, **54**, Haarlem, The Netherlands, 168 p.